RESEARCH ARTICLE | DECEMBER 09 2024

Demonstration of a telecentric lens relay system for PDV in plate-impact experiments

Jasper G. Threadingham ✉; Xuefei Liang; Jeremy C. F. Millett; Glenn Whiteman; David J. Chapman; Daniel E. Eakins

AIP Conf. Proc. 3066, 450015 (2024)
https://doi.org/10.1063/12.0032369

Demonstration of a Telecentric Lens Relay System for PDV in Plate-Impact Experiments

Jasper G. Threadingham,[1, a)] Xuefei Liang,[1] Jeremy C. F. Millett,[2] Glenn Whiteman,[2] David J. Chapman,[1] and Daniel E. Eakins[1]

[1] *Department of Engineering Science, University of Oxford, Oxford, UK*
[2] *AWE, Aldermaston, Reading, UK*

[a)]Corresponding author: jasper.threadingham@eng.ox.ac.uk

Abstract. Photon Doppler velocimetry (PDV) has become a standard diagnostic in impact and shock experiments, due to its relative flexibility and ease in alignment compared to other optical diagnostics. The conventional approach to fielding PDV in plate-impact experiments is to place probes directly down-range from the projectile and target. In experiments such as these, probes are almost certainly destroyed, resulting in significant replacement cost particularly when multiple probes are used. To overcome these shortcomings, a free-space optical relay system has been developed to focus multiple channels of PDV from outside an experimental tank onto a target of reduced size than the probe array. This system has been successfully tested on plate-impact experiments measuring a Hugoniot state of polycrystal tin, and the peak elastic stress and spall strength in 6082 aluminium alloy, in both cases adding information about the shock tilt to the experimental data generated.

INTRODUCTION

First proposed by Strand *et al.* [1, 2], photon Doppler velocimetry (PDV) has become a standard diagnostic fielded in high-rate and shock experiments to measure the motion of a surface in a time-resolved fashion. Based on the Doppler shift of laser light reflected from a moving surface, PDV has been shown to provide a robust and flexible method of measuring velocity in the direction of the probe on a range of surface types, with tailorable velocity sensitivities, and across various timescales depending upon the limiting sampling rate of recording systems [3, 4].

Despite a wide range of configurations, PDV is typically fielded using optical probes or bare fibres to convey laser light to, and collect said light from, the measurement surface over relatively short stand-off distance [3]. While this is a convenient and reliable method of fielding PDV, it can prove costly when fielding multiple probes that are often destroyed in impact tests. Additionally, the size of the probe body used can place physical limits on the spatial arrangement of measurement points on the diagnosed surface.

Optical methods can be used to direct and focus multiple channels of PDV, improving the capabilities of the system at the expense of simplicity. For instance, a significant body of literature [5-10] has been devoted to developing fish-eye lenses to focus multiple channels from a single fibre bundle onto the inner surface of a curved bowl. As the surface implodes under an explosive driver, the collapse can then be measured at a number of points on the surface. In other examples, lens pair systems have be used to extend the distance between probes and the target. In work by Kaufman *et al.* [11], a 1:1 magnification double lens relay is used to remove the probes from the impact axis in gas-gun driven experiments by reflecting the lasers onto the measured surface using a pellicle beamsplitter. This helped avoid a secondary impact with the probes and their mounts, thereby facilitating clean recovery of the target for post-shock analysis. A lens pair system has also recently been used by Yang *et al.* [12] to focus eight channels of PDV onto a line along a target. This system scales-up (magnifies) the array meaning the points on the target are less tightly-packed than at the originating probes. Thus the probes are aligned as a group bundle.

In this paper, we describe an optical relay to focus the output for multiple PDV probes from outside an experimental tank onto a target smaller than the probe array. This means not only are the optical components reused in multiple experiments, but also that the probes can be kinematically mounted and fine-tuned with relative ease compared to an array of the same size as the target. By exploiting a simple 4f double-telecentric design to focus the array of probes, the cost of fielding PDV is reduced, with only a single mirror lost in each experiment. The use of the double-telecentric design also ensures the magnification is unchanged with target stand-off or motion. This array has been demonstrated on two plate-impact experiments, to gather surface velocities from an array of target points of interest, and to simultaneously diagnose impact tilt from differences in shock break-out time.

23rd Biennial Conference of the APS Topical Group on Shock Compression of Condensed Matter
AIP Conf. Proc. 3066, 450015-1–450015-7; https://doi.org/10.1063/12.0032369
Published under an exclusive license by AIP Publishing. 978-0-7354-5080-6/$30.00

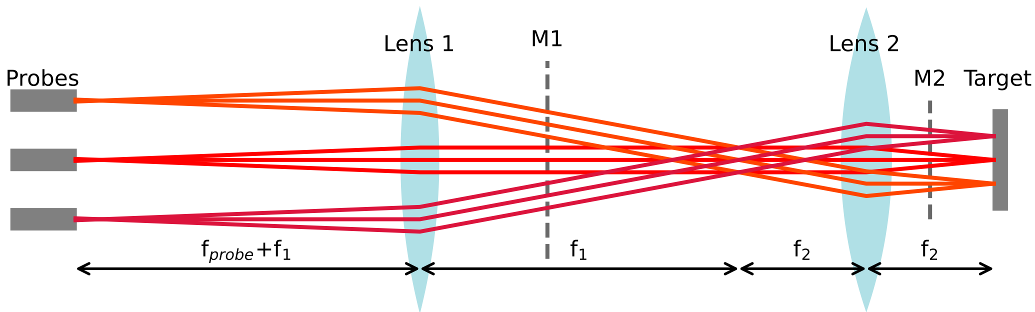

FIGURE 1. Schematic representation of rays in the double-lens PDV relay. By placing the components on their focal lengths, a central region with parallel rays is created between two regions with parallel beams. Symmetry can then be exploited to focus a large array of probes onto a small target. In the real design, mirrors are placed at the marked locations M1 and M2 to remove the components from the path of debris created in the gas-gun experiment.

DOUBLE TELECENTRIC LENS DESIGN

The principle behind a double telecentric lens is relatively simple. By placing lenses and other optical elements spaced by their respective focal lengths (f), a robust relay is produced, shown in Figure 1. Note the parallel beams between the probes and lens 1 and between lens 2 and the target, while between the two lenses the rays in each beam are parallel and unfocused. Due to the symmetry of this central region, using lenses of different focal lengths results in a magnification (target PDV point spacing to probe spacing ratio) given by the ratio of the focal lengths of the two lenses. This design is relatively robust, with an image plane formed reliably in the desired location. The optical axes of the parallel beams are also perpendicular to the target meaning the system is optimally configured to collect sufficient return signal with only minor adjustments. Importantly, the parallelism of probe optical axes minimise relative shifts in measurement location throughout rear surface motion, an issue often associated with non telecentric imaging relays.

Practical setup

The practical setup of this telecentric lens system is shown in Figure 2 prepared for use in a plate-impact experiment on a single-stage gas gun. As shown, a mirror is used behind the target to remove most of the costly components from the path of the gas gun (M2 position in Figure 1). This mirror is mounted on a kinematic mount and a manual linear stage to align the beam path to the target. Due to the dimensions of the array, the second lens and probes can therefore be mounted outside the target tank, requiring a wedged window into the tank to remove back-reflections from the primary beam path. The wedged window and both lenses are all anti-reflective coated for the 1550 nm laser used by the PDV system. A second mirror (M1 position in Figure 1) is used outside the tank so the external components run parallel to the wall of the tank. Cage systems are used to ensure the lenses and probes can easily be moved parallel to the beam path. The probes are mounted in kinematic mounts on a 3D-printed block designed to fit the cage system. This gives a fine degree of angular and spatial positioning. To improve the economy of the design, pigtailed collimators are used instead of focusing probes, with half their ideal coupling length used as the focal length of the probe in Figure 1.

Aligning and visualising the array

Due to the requirement for the optical path to be formed perpendicular and central to the target, aligning the system requires two main steps. Firstly, the cages and mirrors are aligned to a laser shone centrally down the barrel from the breech end. The spacing of the lenses and probes are taken along this laser path. After this the lenses and target are mounted, and the radial probes fine-tuned to ensure a return path.

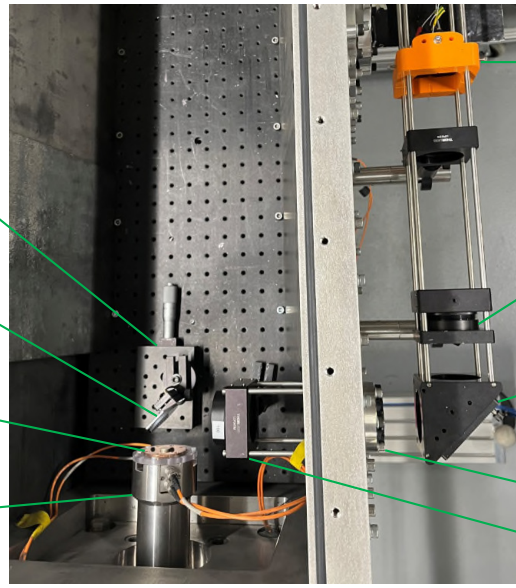

FIGURE 2. Picture of practical setup mounted onto a single-stage gas gun target tank.

By following these steps, the probes are reliably aligned to the centre of the target. However to ensure the PDV probes are correctly positioned, and in order to measure the spacing for the tilt analysis, the position can be visualised. To do this, two methods can be used. The simplest method to visualise the laser points is to use a visible-light laser, rather than the 1550 nm wavelength of standard PDV. However, the refractive index of the fused silica lenses varies with wavelength, meaning the paths are different for each wavelength. Alternatively, a pellicle beamsplitter can be inserted into the beam path, and a camera sensitive to both visible and infrared light used. While the beamsplitter will perturb the beam path slightly, this system allows for head-on visualisation as shown in Figure 3b. From this image the pitch circle diameter of the radial probes can be measured, with the result of 13.5 mm in the example shown, corresponding to the probe pitch circle diameter multiplied by the magnification.

EXPERIMENTAL APPLICATION

Plate impact experiment to measure a Hugoniot state of tin

The telecentric PDV imaging system has been demonstrated on two separate plate impact experiments showcasing its utility in measuring impact tilt and shock state, as well as detecting the onset of radial release. A “top hat” geometry with a C101 copper driver and 5N tin sample is shown in Figure 3a. The three radial probes have been used to quantify the arrival time in the tin, as well as the arrival tilt, while the central probe was used on the rear surface of the tin to measure break out, with the resulting velocity histories calculated using the short-time Fourier transform approach and plotted in Figure 4a. From this, the shock wave speed and particle velocities can be determined, enabling other state information including the density and pressure to be calculated using the Rankine-Hugoniot jump conditions [13]. Assuming the isentrope does not significantly deviate from the Hugoniot, the internal particle velocity is half the peak release velocity on the free surface, with Figure 4a giving an internal particle velocity of 543 $\mathrm{m\,s^{-1}}$. Taking arrival times from the 50 % threshold of each wave, and taking the mean arrival time of the radial copper probes gives a shock wave speed of 3330 $\mathrm{m\,s^{-1}}$. An initial density of 7.29 $\mathrm{g\,cm^{-3}}$ results in a pressure of 13.2 GPa and a relative volume of 0.837. This pressure-volume pair is plotted alongside literature values in Figure 4b. Similarly, the shock arrival times can be found on the copper driver using the radial probes. These can be directly used to determine the tilt of the shock wave as it enters the sample [14], which in this case is found to be 3.1 mrad.

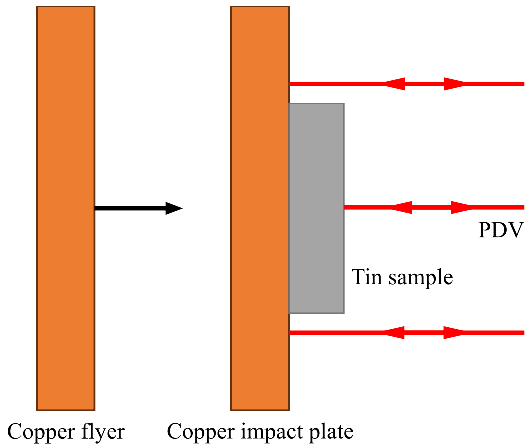

(a) Schematic geometry of the top hat experiments, showing the copper flyer striking a copper impact plate to enable a Hugoniot state measurement in the tin sample

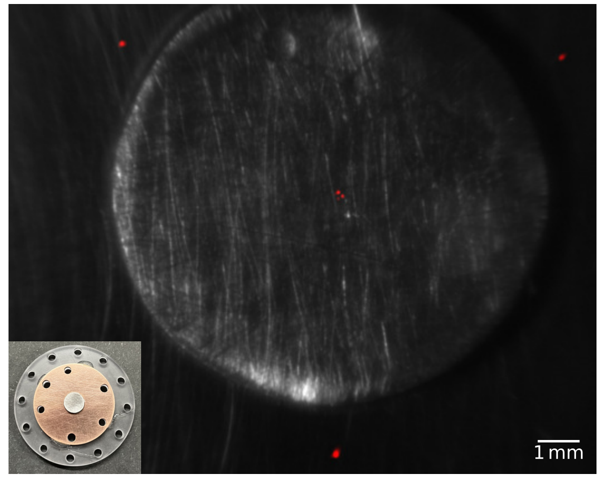

(b) A composite image visualising the PDV points (recoloured red) on a "top-hat" sample using a camera sensitive to visible light and 1550 nm. The central probe on the sample (⌀11.00 mm) and three radial probes focused on the driver plate can be seen. An image of the target on the barrel-interface plate is inset.

FIGURE 3. A top hat experiment can be used to measure the shock wave speed and magnitude in order to determine Hugoniot state information. Knowing the spacing of the PDV points is key to measuring the impact tilt.

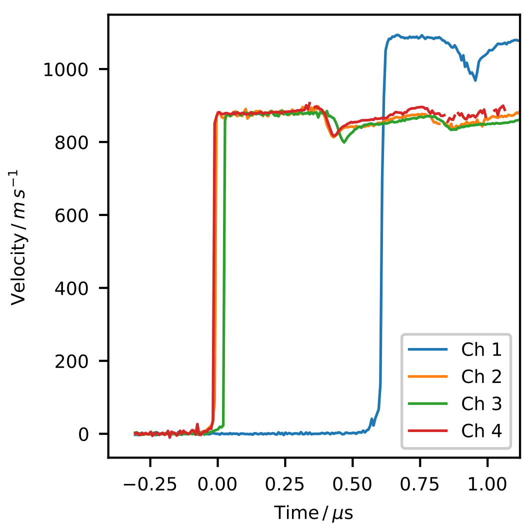

(a) PDV velocity traces, with Ch1, the central channel, showing the breakout on rear surface of the tin sample, and channels 2-4 showing the radial breakout on a copper transmission plate. The impact tilt can be determined from the relative timing between these radial channels.

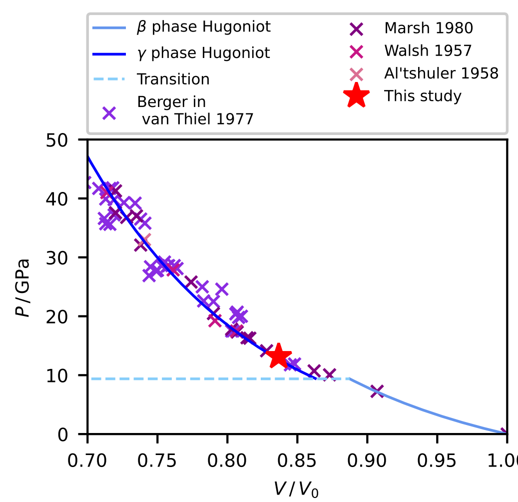

(b) Pressure vs. relative volume data determined experimentally using the PDV relay compared to literature values [15-18]. The Hugoniot shown is calculated from Birch-Murnighan parameters published by Mabirre and Héreil [19].

FIGURE 4. Experimental data from a "top-hat" plate-impact experiment of a polycrystal tin sample.

Plate impact experiment to measure the shock properties of an aluminium alloy

In order to further demonstrate the viability of the telecentric PDV image relay, we also present velocity histories obtained during a typical spall experiment. The relative dimensions were chosen to cause radial release of the outer radial array of 3 probes and hence challenge the optical efficiency. The spall experiment employed a symmetric impact of Al 6082-T6 aluminium alloy, and the impact speed is $353\,\mathrm{m\,s^{-1}}$. From the PDV data, the peak elastic stress σ_E, initial plastic strain rate of shock $\dot{\varepsilon}_p$ [20], spall strength σ_{spall} and spall pullback strain rate $\dot{\varepsilon}_s$ can be calculated based on the rear surface velocity [21-23] .

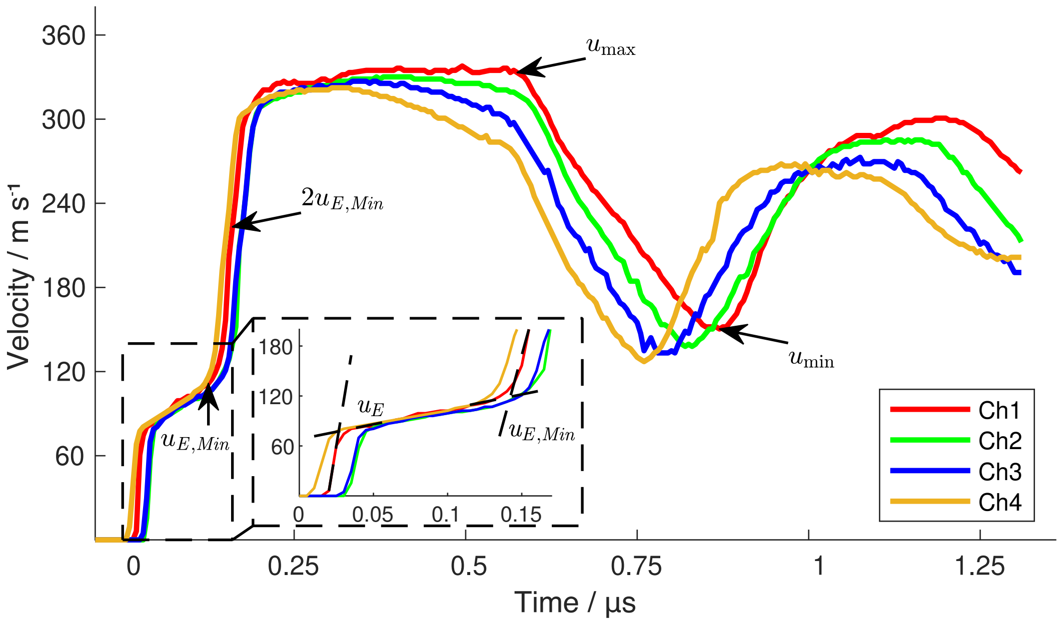

FIGURE 5. PDV velocity traces, with Ch1-4 showing the velocity of rear surface of Al6082-T6. The Ch1 shows the central channel. Due to lateral release from the edge of the sample, the three radial probes, Ch2-4, detect release earlier than the center signal Ch1.

The rear surface velocity is shown in Figure 5. Due to the tilt of the impact, the four probes detect the arrival time in sequence, with the tilt found to be 0.75 mrad. Taking a literature value of density for Al6082 alloy of $2.70\,\mathrm{g\,cm^{-3}}$ and longitudinal sound speed of $6400\,\mathrm{m\,s^{-1}}$ [28], gives a Hugoniot elastic limit of 0.68 GPa. The time taken for the change of particle velocity from $u_{\mathrm{E,Min}}$ to $2u_{\mathrm{E,Min}}$ during the main shock wave gives an initial plastic strain rate of $4.98\times10^5\,\mathrm{s^{-1}}$ following the approach of Smith *et al.* [20]. These results are plotted against literature values in Figure 6a.

In addition to the differences in the arrival time of the elastic precursor, it is also noted that the release from the peak shock state is different between all four probes, due to the three radial probes detecting the lateral release at different times. This serves to demonstrate the robustness of the optical relay to non-planar motion, where despite the lengthened optical path, adequate signal collection was maintained. The central channel, channel one, was in the centre of the sample where lateral release would arrive the latest at $\sim$1.81 µs, long after the signature of spall following longitudinal release has arrived at the free surface. Analysing the spall pull back, the initial rear-surface velocity is $336\,\mathrm{m\,s^{-1}}$, dropping to a minimum of $150\,\mathrm{m\,s^{-1}}$, giving a spall strength [29, 30] of 1.75 GPa and a spall pullback strain rate [22, 23] of $4.56\times10^4\,\mathrm{s^{-1}}$. Due to a lack of literature data of Al6082-T6 spall, these results are compared to spall data for Al6061-T6, an aluminium alloy with a very similar composition and therefore mechanical properties to Al6082-T6, calculated by Grady [27]. The definition of strain rate used by Grady is determined by the approximate pulse duration at the flyer-sample interface, which in the case of the experimental results presented here, is found to be $8.4\times10^4\,\mathrm{s^{-1}}$, shown in Figure 6b. It is found that the Al6082-T6 material has a higher spall strength than Al6061-T6 at the same strain rate.

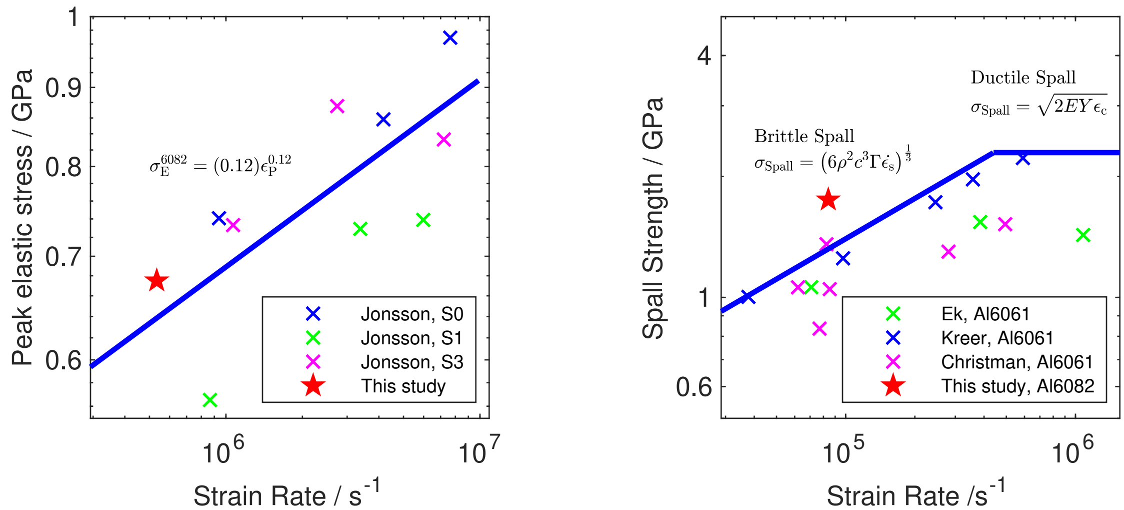

(a) Peak Hugoniot elastic stress in Al 6082 plotted against strain rate. S0, S1 and S3 refer to specimens that have been rotary swaged zero, once and three times respectively, as measured by Jonsson [14].

(b) Spall strength for Al6082-T6 as a function of strain-rate from Al6061-T6 literature [24-26] presented in [27]. Spall strength fits based on the results of Grady [27].

FIGURE 6. Data from plate-impact spall experiments with an aluminium alloy sample.

CONCLUSION

A powerful but economical method of fielding multiple channels of PDV on small targets in gas gun-driven experiments has been demonstrated. This system uses a pair of lenses in a double-telecentric style design to relay and focus an array of probes onto the target, enabling multiple probes to be kinematically mounted outside the experimental tank. This enables the measurement of surface velocity on multiple points on the target, giving a wealth of data, including impact tilt, surface and shock speed velocities. By demonstrating these capabilities on a "top-hat" plate impact, a Hugoniot state measurement was made, while spall experiments using this system measured the peak elastic stress and spall strength. As a result, this approach has the capacity to be a beneficial development for conventional PDV systems in a wide range high-velocity experiments beyond the plate impact equation of state measurement and spall strength determination demonstrated here.

ACKNOWLEDGMENTS

This work would not have been possible without the assistance of Stuart Carter and the ISML workshop for help adapting the target tank to mount the array. The authors also gratefully acknowledge AWE for their continued support.

REFERENCES

1. O. T. Strand, L. V. Berzins, D. R. Goosman, W. W. Kuhlow, P. D. Sargis, and T. L. Whitworth, "Velocimetry using heterodyne techniques," (SPIE, 2005) p. 593.
2. O. T. Strand, D. R. Goosman, C. Martinez, T. L. Whitworth, and W. W. Kuhlow, "Compact system for high-speed velocimetry using heterodyne techniques," Review of Scientific Instruments **77** (2006).
3. O. T. Strand, "Handbook for the photonic Doppler velocimeter," (2020).
4. D. H. Dolan, "Extreme measurements with photonic Doppler velocimetry (PDV)," Review of Scientific Instruments **91** (2020).
5. R. M. Malone, M. E. Briggs, B. M. Cata, B. C. Cox, E. P. Daykin, D. O. DeVore, D. L. Esquibel, D. K. Frayer, B. C. Frogget, M. R. Furlanetto, C. H. Gallegos, D. B. Holtkamp, M. I. Kaufman, K. D. McGillivray, P. Pazuchanics, L. E. Primas, V. T. Romero, M. A. Shinas, and D. S. Sorenson, "Design, assembly, and testing of a photon Doppler velocimetry probe," (SPIE, 2011) p. 813109.

6. R. M. Malone, B. M. Cata, E. P. Daykin, D. L. Esquibel, B. C. Frogget, D. B. Holtkamp, M. I. Kaufman, K. D. Mcgillivray, M. J. Palagi, P. Pazuchanics, V. T. Romero, and D. S. Sorenson, "Photonic Doppler velocimetry probe designed with stereo imaging," Proceedings of SPIE - The International Society for Optical Engineering **9195**, 919503 (2014).
7. R. M. Malone, M. I. Kaufman, D. K. Frayer, K. D. McGillivray, S. A. Clarke, S. J. Fensin, and D. R. Jones, "Photonic Doppler velocimetry probe used to measure grain boundaries of dynamic shocked materials," (SPIE-Intl Soc Optical Eng, 2017) p. 3.
8. B. C. Frogget, B. M. Cata, B. C. Cox, D. O. DeVore, D. L. Esquibel, D. K. Frayer, M. R. Furlanetto, D. B. Holtkamp, M. I. Kaufman, R. M. Malone, and V. T. Romero, "A fisheye lens as a photonic Doppler velocimetry probe," (SPIE, 2012) p. 84940D.
9. B. C. Frogget and V. T. Romero, "US20140118719A1," (2014).
10. J. R. Danielson, E. P. Daykin, A. B. Diaz, D. L. Doty, B. C. Frogget, M. R. Furlanetto, C. H. Gallegos, M. Gibo, A. Garza, D. B. Holtkamp, M. S. Hutchins, C. Perez, M. Peña, V. T. Romero, M. A. Shinas, M. G. Teel, and L. J. Tabaka, "Measurement of an explosively driven hemispherical shell using 96 points of optical velocimetry," (Institute of Physics Publishing, 2014).
11. M. I. Kaufman, R. M. Malone, B. C. Frogget, D. L. Esquibel, V. T. Romero, G. A. Lare, B. Briggs, A. J. Iverson, D. K. Frayer, D. DeVore, B. Cata, D. B. Holtkamp, M. D. Wilke, N. S. P. King, M. R. Furlanetto, M. E. Briggs, and M. D. Furnish, "Design, construction, alignment, and calibration of a compact velocimetry experiment," (SPIE, 2007) p. 667607.
12. J. Yang, Y. Yan, Q. Li, G. Shi, Z. Wang, Y. Zhang, S. Zhang, and J. He, "Design of spatial resolution PDV probe based on double telecentric lens," Guangzi Xuebao/Acta Photonica Sinica **50** (2021).
13. J. W. Forbes, *Shock Wave Compression of Condensed Matter*, 1st ed. (Springer Berlin, Heidelberg, 2012).
14. J. C. Z. Jonsson, "Studies on the role of microstructure in the dynamic strength of metals," (2021).
15. S. P. Marsh, "LASL shock hugoniot data," (1980).
16. J. M. Walsh, M. H. Rice, R. G. Mcqueen, and F. L. Yarger, "Shock-wave compressions of twenty-seven metals. equations of state of metals," Physical Review **108** (1957).
17. L. V. Al'tshuler, K. K. Krupnikov, and M. I. Brazhnik, "Dynamical compressibility of metals under pressure from 400000 to 4 million atmospheres," Soviet Physics JETP **34** (1958).
18. M. van Thiel, "Compendium of shock wave data," (1977).
19. C. Mabire and P. L. Héreil, "Shock induced polymorphic transition and melting of tin," AIP Conference Proceedings **505**, 93–96 (2000).
20. R. F. Smith, J. H. Eggert, R. E. Rudd, D. C. Swift, C. A. Bolme, and G. W. Collins, "High strain-rate plastic flow in Al and Fe," Journal of Applied Physics **110**, 123515 (2011).
21. G. I. Kanel, "Dynamic strength of materials," (1999).
22. G. V. Stepanov, "Spalling produced by elastoplastic waves in metals," Strength of Materials , 66–70 (1966).
23. V. I. Romanchenko and G. V. Stepanov, "Dependence of the critical stresses on the loading time parameters during spall in copper, aluminum, and steel," Journal of Applied Mechanics and Technical Physics **21**, 555–561 (1980).
24. J. R. Kreer, "Dynamic fracture in 6061-T6 aluminum," (1971).
25. D. R. Christman, W. A. Isbell, S. G. Babcock, A. R. McMillan, and S. J. Green, "Measurements of dynamic properties of materials volume III 6061-T6 aluminum," (1971).
26. D. R. Ek and J. R. Asay, "The stress and strain-rate dependence of spall strength in two aluminum alloys," (1986).
27. D. E. Grady, "The spall strength of condensed matter," Journal of the Mechanics and Physics of Solids **36**, 353–384 (1988).
28. J. C. Millett, G. Whiteman, and N. K. Bourne, "Lateral stress and shear strength behind the shock front in three face centered cubic metals," Journal of Applied Physics **105** (2009).
29. D. E. Grady, "Steady-wave risetime and spall measurements on uranium (3-15 GPa)," (1986).
30. D. Grady, *Physics of Shock and Impact*, Vol. 1 (IOP, 2017).